AD-785 266

MOLDING OF ORIENTED SHORT-FIBER COMPOSITES. IV. CHARACTERIZATION OF FIBER ORIENTATION PATTERNS

Lloyd A. Goettler

Monsanto Research Corporation

Prepared for:

Office of Naval Research
Advanced Research Projects Agency
Washington University

August 1974

DISTRIBUTED BY:

NTIS

National Technical Information Service
U. S. DEPARTMENT OF COMMERCE
5285 Port Royal Road, Springfield Va. 22151

AD-785 266

Security Classification

DOCUMENT CONTROL DATA - R & D

(Security classification of title, body of abstract and indexing annotation must be entered when the overall report is classified)

1. ORIGINATING ACTIVITY *(Corporate author)* Monsanto Research Corporation	2a. REPORT SECURITY CLASSIFICATION Unclassified 2b. GROUP

3. REPORT TITLE

Molding of Oriented Short-Fiber Composites. IV. Characterization of Fiber Orientation Patterns.

4. DESCRIPTIVE NOTES *(Type of report and inclusive dates)*

5. AUTHOR(S) *(First name, middle initial, last name)*

Lloyd A. Goettler

6. REPORT DATE	7a. TOTAL NO. OF PAGES	7b. NO. OF REFS
August, 1974	40	7

8a. CONTRACT OR GRANT NO b. PROJECT NO. c. d.	9a. ORIGINATOR'S REPORT NUMBER(S) HPC 72-151 9b. OTHER REPORT NO(S) *(Any other numbers that may be assigned this report)*

10. DISTRIBUTION STATEMENT

Approved for public release; distribution unlimited

11. SUPPLEMENTARY NOTES	12. SPONSORING MILITARY ACTIVITY Office of Naval Research Washington, D. C.

13. ABSTRACT The various considerations underlying the specification and characterization of three-dimensional orientation distributions in moldings of short fiber reinforced polymers are discussed. The recommended treatment resolves the overall complex orientation pattern into distributions on a macroscopic and microscopic scale.

Some examples, including the effects of molding conditions, are given for an end-gated rectangular bar plunger molded from fiberglass reinforced epoxy.

DD FORM 1 NOV 65 1473 (PAGE 1)

S/N 0101-807-6801

Security Classification

Security Classification

14. KEY WORDS	LINK A		LINK B		LINK C	
	ROLE	WT	ROLE	WT	ROLE	WT
Composite						
Fiberglass						
Epoxy						
Fiber orientation						
Molding						
Flow rate						
Orientation distribution						
Orientation measurement						
Angle						
Viscosity						
Gate						
Variance						

DD FORM 1 NOV 65 1473 (BACK)
(PAGE 2)

Security Classification

HPC 72-151 Item A002

MOLDING OF ORIENTED SHORT-FIBER COMPOSITES
IV. CHARACTERIZATION OF FIBER ORIENTATION PATTERNS

by

Lloyd A. Goettler

Monsanto/Washington University Association
High Performance Composites Program

Sponsored by ONR and ARPA
Contract No. N00014-67-C-0218, ARPA Order 876

FOREWORD

The research reported herein was conducted by the staff of Monsanto/Washington University Association under the sponsorship of the Advanced Research Projects Agency, Department of Defense, through a contract with the Office of Naval Research, N00014-67-C-0218 (formerly N00014-66-C-0045), ARPA Order No. 876, ONR contract authority NR 356-484/4-13-66, entitled, "Development of High Performance Composites."

The prime contractor is Monsanto Research Corporation. The Program Manager is Dr. Rolf Buchdahl (Phone 314-694-4721).

The contract is funded for $7,000,000 and expires 30 June, 1974.

Molding of Oriented Short-Fiber Composites

IV. Characterization of Fiber Orientation Patterns

by

Lloyd A. Goettler

ABSTRACT

The various considerations underlying the specification and characterization of three-dimensional orientation distributions in moldings of short fiber reinforced polymers are discussed. The recommended treatment resolves the overall complex orientation pattern into distributions on a macroscopic and microscopic scale.

Some examples, including the effects of molding conditions, are given for an end-gated rectangular bar plunger molded from fiberglass reinforced epoxy.

This research was supported by the Advanced Research Projects Agency of the Department of Defense and was monitored by the Office of Naval Research under Contract No. N00014-67-C-0218.

√

Molding of Oriented Short-Fiber Composites
IV. Characterization of Fiber Orientation Patterns

by

Lloyd A. Goettler

Introduction

Injection or transfer molding is an economical means for the large scale fabrication of hardware from fiber reinforced thermosetting polymers. The resulting orientation distribution of individual fibers that is produced by the flow is one of the major factors determining the mechanical strength as well as stiffness of the molded part. Fiber orientation can be controlled by changing the flow geometry and molding conditions (3,6,7). By centering the orientation distribution around the direction of the applied stress, threefold improvements in strength and stiffness are possible.

Here we consider the different methods that can be used to characterize and measure an orientation distribution in two simple molded pieces. Diverging flow through a small end gate produces a predominantly transverse fiber orientation in a rectangular bar. In contrast, a high degree of axial fiber alignment can be produced by filling a rod cavity through a conical converging section attached to one end. These geometries and the resulting fiber orientation patterns are illustrated in Figure 1.

In addition, changes in the orientation distribution obtained in the conventionally end-gated rectangular bar due to the effects of molding conditions are described as an extension of the work previously reported (1,3).

The necessary calculations to convert measurements of fiber directionality into orientation parameters also are described. However, the prediction of mechanical response from a known or measured orientation distribution is treated separately elsewhere (2).

Orientation Characterization in Rectangular Moldings.

The mechanical response of a fiber reinforced composite subjected to a unidirectional stress is governed by the distribution of polar angles (θ_1) that describe each fiber's direction relative to the stress axis. Since this distribution is difficult to measure directly, a simpler but still meaningful method, involving the measurement of planar angles, was developed. The angles ϕ_2 and ϕ_3 are measured in orthogonal planes that include the axis, and these are then combined to calculate the average polar angle for the molding. These angles are defined in Figure 2; the 1-axis is selected as the direction of stress.

The distributions of the planar angles themselves are further resolved into local means $\bar{\phi}_2$ and $\bar{\phi}_3$, which are smoothed functions of coordinate position in the part, and the local distributions of individual fibers around these mean directions. That is, the distributions of the fibers are taken to be normal (the measured distributions are bell-shaped and symmetrical) with mean $\bar{\phi}_2(x_1, x_2, x_3)$ or $\bar{\phi}_3(x_1, x_2, x_3)$ and standard deviation s_2 or s_3, where x_1, x_2, x_3 are the axes of a rectangular coordinate system. The variables are defined for the example of an end-gated rectangular bar in Figure 3.

As described in (1), the macroscopic orientation patterns $\overline{\phi}_2$ and $\overline{\phi}_3$ are determined by fitting a multilinear regression equation to angular measurement of the local mean fiber direction made from 6x photographs of polished surfaces cut into the moldings. The fiber patterns are contrasted against the matrix by etching the partially bundled glass fibers with hydrofluoric acid and filling the pits with an ink or dye. Angle measurements are made at predetermined mesh points using the protractor arm of a drafting machine. A smooth multilinear curve for $\overline{\phi}_2$ or $\overline{\phi}_3$ as a function of coordinate position is fit to these measurements by a regression technique. This allows an overall average to be taken over the dimensions of the molding.

The standard deviations consist of two components: the deviation of the individual fiber orientations, s_F, about the local mean in a small region about a point in the molding and the standard error, s_R, of the smoothed multilinear regression fit of $\overline{\phi}(x_1, x_2, x_3)$ to the measurements of local $\overline{\phi}$. The term s_R^2 characterizes the macroscopic variance in a molded part, which must be added to the microscopic individual fiber variance s_F^2 to yield the overall variance in fiber angle

$$s'^2_{2 \text{ or } 3} = (s_F^2 + s_R^2). \qquad (1)$$

This equation is valid as long as the total number of measurements of $\overline{\phi}$ is large. When Equation (1) is used to experimentally evaluate the overall orientation variance, the error, which does not relate to the actual dispersion of the fiber distribution, must be subtracted out:

$$s_{2\,or\,3} = (s_F^2 + s_R^2 - s_M^2) \qquad (2)$$

where s_M^2 is the variance due to measurement error. A chart of the orientation calculation process illustrating this flow of variance is given in Figure 4. The standard error of regression, s_R, of course would not be expected to be identical for $\overline{\phi}_2$ and $\overline{\phi}_3$ in a given sample, although wide deviations do not occur.

Since the individual fiber dispersion, s_F, is found to be approximately constant within a given molding, it is taken to be independent of coordinate position in the calculations. However, s_F does depend upon the material and molding conditions. For example, s_F is lower in moldings that start with a tighter, harder bundle in the molding compound. Some typical values are given in Table 1.

The distributions of individual fiber directions needed to determine the standard deviations s_F could be measured from polished unetched surfaces at 500x magnification. Since s_F is relatively constant, only a few sets of these need be made for each molding to be analyzed.

The measurement error, s_M, has been assessed by making multiple determinations of the same field. It varies from 8 to 20° and depends primarily on the clarity of the photograph of the polished molding surface. An average value is 10°. Errors associated with the alignment of the fields in the photographs and the determination of the measurement locations are negligible in comparison to the major error source of determining the directionality of the orientation pattern at those points.

This method is believed to conceptually simplify the study of orientation by separating the types of variation into microscopic and macroscopic categories. In addition, it inherently considers the positions of a great many fibers in determining the orientation direction, but requires a relatively small number of measurements on individual fibers to determine s_2 and s_3. For these reasons, it is preferred to the alternate procedures of tediously measuring the polar angles of many individual fibers or of only a few tracer fibers. The method is practical, but not exact. It does, however, accomplish the task of analyzing the intermeshed network of fibers that exists in the moldings.

A knowledge of the complete fiber orientation distribution with respect to the direction of applied uniaxial stress is required for determining the dependence of mechanical properties on fiber direction. This is provided when $\bar{\phi}_2$, $\bar{\phi}_3$, s_2 and s_3 are all specified. Previously, a method of integrating a directional mechanical property over the orientation distribution was described (2) for prediction of the modulus of molded bars. However, in other cases it is convenient to merely indicate the degree of directionality in a piece by an overall average angle, $\bar{\bar{\theta}}_1$, which can be calculated in a similar manner. Since θ_1 only takes on values on the range $0 \leq \theta_1 \leq 90°$, its average, $\bar{\bar{\theta}}_1$, is a measure of the degree of dispersity in fiber orientation centered about the 0° or 90° direction. For example, $\bar{\bar{\theta}}_1$ can equal zero only in composites that are perfectly aligned in the stress direction.

In the regression analyses for $\bar{\phi}_2$ or $\bar{\phi}_3$, a smooth curve can be obtained across the centerline only if the algebraic rather than absolute angle measurements are used. Then, although an angle of $+\beta°$ will cancel with one of $-\beta°$ to yield an average angle of 0°, the difference from a well-aligned composite will show up in the finite standard deviation. Further, in order to allow the distributions about the regression line to remain symmetric over the entire domain of -90 to +90°, the angle range is allowed to extend from -135° to +135°. Angles of $(90 + \alpha)$ are, of course, equivalent to $-(90 - \alpha)$.

This problem of duplicity of values occurs because the polar distribution is being treated by linear statistics that assume an infinite domain of $-\infty$ to $+\infty$ for the independent variable. A more correct method would be to determine the position of the centroid on a polar representation of the distribution as in

Figure 5. Because the fiber ends are indistinguishable, the circle need cover only 180 instead of 360°. The length ρ of the radius vector in such a plot represents the frequency of occurrence of the indicated angle. However, the statistics of such a treatment would be more involved. The artificial implementation of overlapping linear domains will suffice to prevent the occurrence of anomalous mean values such as 0° for the symmetric distribution illustrated in Figure 5.

When the orientation distribution in a molded piece is symmetric about one or more planes, the correlation of macroscopic angles entering into $\overline{\Phi}_{2\text{ or }3}$ can be confined to the half-plane. The range of angles can then be restricted to $-45° < \phi < 135°$. If the orientation at the center is transverse, as will occur if a long molding is end-gated through a small gate, the angles ϕ_2 and ϕ_3 , as defined in Figure 3, will both be zero at the centerline.

Figure 6 shows orientation patterns in a polished plane cut through the midsection ($x_2 = 0$) of the 1/4" x 1" x 6" bar previously described in Figure 3. In this case, the pattern was made to appear by adding a small amount of carbon black nonuniformly to the molding compound. It is identical to the pattern produced by the etch-dying technique described earlier. Flow is from bottom to top in the picture, and the fibers are laying parallel to the black streaks. There is an almost completely transverse fiber orientation throughout most of the core, surrounded by an envelope of predominantly longitudinal orientation. The angle measurements can be fitted by a cubic of the form

$$\overline{\phi}_2 = (a_1 + b_1 x_2^2)x_3 + a_2 x_3^2 + a_3 x_3^3 \quad . \qquad (3)$$

The distance coordinates were normalized to range from zero at the center of the molding to unity at the edges of the bar.

Measurements made from such photographs have been shown to represent the local average fiber orientation on the microscopic level. The statistical hypothesis that these two quantities are identical can be accepted at a level of significance $\alpha = 0.10$ with a power of 0.99 against the alternate hypothesis that they differ by 5°. In a more expanded form of Equation (3) the coefficients are not all statistically significant. When the orientation pattern does not contain an inflection point a simpler quadratic fit will suffice.

The corresponding graph of the planar orientation $\overline{\phi}_2$ in the central horozontal plane $x_2 = 0$ is given in Figure 7. At the same x_3, the variations of ϕ_2 between parallel x_2 planes are small, being less than 5°. (A higher alignment in the flow direction occurs near the upper and lower surfaces.) According to the definition of angles used, 0° corresponds to a transverse orientation and 90° is directed along the length of the bar. In this figure the 90% confidence envelope of $\pm$ 3° to 6° is indicated by dashed lines. The prediction interval, i.e., the envelope in which there is a 90% probability that a measured $\overline{\phi}_2$ will fall, is considerably larger (26°). By reproducing additional moldings under the same set of molding conditions it was found that the hypothesis that all sample orientation distributions came from the same parent population could be accepted at a significance level of $\alpha = 0.20$. Thus, 98% of the observed overall variance arose within the individual samples rather than deriving from differences between them.

It should be noticed that no dependence on x_1 is indicated by Equation (3). Although changes in $\bar{\phi}_2$ of 7° at the middle of the half-plane ($x_3 = 0.5$) and 13° near the wall occurred in some samples, this small change was not statistically significant. For example, the hypotheses that the regression coefficients on the x_1 terms that would be added to Equation (3) are equal to zero could be accepted at the very high significance level of 0.8. On the average, an axial change of 2°/inch of bar was found for the region excluding 0.5" at the gate end and 1.0" at the vent end where end effects were prevalent.

One might expect that with a smaller cross-sectional dimension, shearing stresses would develop within the fiber mass, and orientation would thus vary with flow distance in uniform channels. However, in highly concentrated suspensions, the region of shear usually maintained within a thin (< .2 mm) layer of pure resin at the wall so that orientation patterns remain stationary in shear flows.

Some Orientation Profiles for Molded Bars.

The example of an orientation profile of the local mean planar angle $\overline{\Phi}_2(x_3)$ shown in Figure 7 can be used as a semi-quantitative indication of the type and level of orientation in the molded 1/4" x 1" x 6" bar. The bar analyzed for this figure was molded through a large 1/8" x 1/2" end gate from a high viscosity epoxy that was 58% reacted in the B-stage. This molding compound contained 1/8" E-glass fibers (Johns Manville, type CS308A chopped strand) at 40% volume concentration. The molding compound was made by a technique that utilized a suspension of fibers in an aqueous emulsion of epoxy and water (4). Although concise grains of fiber-filled molding compound were formed, water was occluded and the degree of B-stage was high (56-62% of epoxide units reacted). The response of this material to different gate geometries and molding conditions has been described (1,3).

A material with only 40% reacted epoxides in the B-stage can easily be made by hand-blending the fibers into activated liquid epoxy resin at 60°C. A reasonable degree of wetting is accomplished, and definite though imperfect grains of molding compound can be produced by the blending process. Details of the preparative techniques are given in (5). Figure 8 shows the relationship between the fraction of epoxide groups reacted and the matrix viscosity, as measured in a falling ball viscometer. With the stoichiometric ratio of epoxy and MDA curing agent used in these studies, a 50% conversion of epoxide corresponds to a completely linear molecular structure. Further reaction involves the onset of crosslinking.

The response of this material to changes in gate geometry, resin viscosity (degree of reaction in the B-stage), flow rate, fiber length and bundle integrity are discussed below. Since the basic geometry is a bar end-gated through a small gate, the expansion in cross-sectional area will cause an internal core of transverse fibers. The changes in molding conditions will be seen to only affect the degree of longitudinal orientation in the outer envelope and the size of that variable region.

As in the case of the more highly reacted and, consequently, higher viscosity material reported in (3), there is no effect of fill rate on orientation with edge gates equal to or smaller than 1/4" x 0.060". However, a lesser degree of transverse orientation is obtained when the resin viscosity is lower. The variation of $\bar{\phi}_2(x_3)$ w ch degree of reaction of epoxide groups in the B-stage is shown in Figure 9. In this case, the change in orientation could result from the greater inertial effect that occurs when a material of lower viscosity squirts through a small orifice. However, Figure 10 shows that the lower viscosity stock also produces a considerably less transverse orientation when a large gate is used. This result relates to the decreasing degree of transverse orientation with increasing mold temperature previously reported in (B). The molding compound viscosity would be lower at the higher temperature.

Figure 10 also compares the orientation produced by a 40% reacted material flowing through a 1/8" x 1/2" gate with that obtained for the smaller gate of Figure 9. The fill rate in this case is 1.9 in^3/min. At higher fill rates the two gates produce a comparable orientation distribution. Figure 11 shows the effect of fill rate with the larger 1/8" x 1/2" gates. As with the higher viscosity material studied in (3), the slow rate of flow produces a higher overall orientation angle (less transverse).

When the sizing is burned off the glass fiber bundles before blending with the liquid epoxy resin for improved wet-out, it is found that there is no change in the orientation pattern. This is surprising since the bundles without sizing open up more during flow into the mold cavity. There is also no change when 1/4" fibers are used instead of the usual 1/8" fiber length.

Orientation Characterization in Rods.

Rods of 1/4" to 1/2" diameter and 6" in length were filled through a converging conical channel attached to one end, which served to orient the fibers into the flow direction by effectively stretching the molten material as it flowed into the mold cavity. Hence, a higher degree of longitudinal orientation than in the bars was obtained without the presence of a transverse core.

The description of orientation patterns in these end-gated rods is simplified by the axial symmetry. The x_1 direction is still taken in the direction of flow; by convention x_2 is the direction of possible shear, which is now radial. Then the x_3 plane is one of constant angle in a cylindrical coordinate system centered along the rod axis. This is a longitudinal plane cut through on a diameter of the cross-section. Since all of these are alike, only one need be measured and the dependence of $\bar{\Phi}_3$ on x_3, which had to be considered for the bars, may be eliminated. However, the x_2 plane in this case is not a flat plane, but a cylindrical surface of constant radius. Not only can orientation patterns not be easily measured on this curved surface, but no smoothed macroscopic variations in orientation in fact even occur, because of the requirement for circular symmetry. A mean constant value of $\bar{\Phi}_2$ could be determined, but this and the measurement of the macroscopic fluctuations that enter into s_R would, as mentioned, be difficult to perform.

Instead, the x_1 plane (rod cross-section) is used in conjunction with the x_3 plane to calculate $\bar{\theta}_1$ according to

$$\bar{\theta}_1(x_2) = \int_{-\infty}^{\infty}\int_{-\infty}^{\infty} \tan^{-1}(\tan\phi_3/\cos\phi_1)N(\bar{\Phi}_3,s_3)N(\bar{\Phi}_1,s_1)d\phi_3 d\phi_1 \quad , \qquad (4)$$

where the N are normal distributions. This is similar to the equation used in reference (2) for the combination of the x_2 and x_3 planes, except that here $\tan\theta_1 = \tan\phi_3/\cos\phi_1$. As in the case of the bars treated above, moldings of sample rods showed no significant variation of orientation in the flow direction (x_1). Consequently, a single cross-sectional plane sufficiently removed from the gate and vent to obviate end effects, would suffice for measurement of $\bar{\Phi}_1$. A convention that 0° implies a radial and 90° a circumferential orientation was adopted. The measurements of $\overline{\phi}_1(x_2)$ and $\overline{\phi}_3(x_2)$ were carried out on photographs of polished surfaces taken at a low magnification to indicate principal directions, as in the treatment of the bar geometry. Individual fiber deviations about the local mean were also found to be about 13°, the same for both planes and similar to values obtained in the bars and reported in Table 1.

Although the $\overline{\phi}_3$ distribution was symmetric, the fibers at the center were no longer restricted to a transverse position, as in the transverse core of the bar previously described. It was therefore no longer proper to require that $\overline{\phi}_3(0) = 0$. A quadratic form for the regression analysis could be substituted for the previous cubic. The variation in $\overline{\phi}_1$, however, could be adequately described by a linear equation. This angle in the cross-section varied from a predominantly radial position near the axis to a circumferential one at the surface.

The averaging over the cross-sectional area to obtain either an overall axial angle $\overline{\overline{\theta}}_1$ or the effective mechanical properties is, because of symmetry, done only along the x_2 or radial direction. A weighting factor must be used to account for the nonlinear relationship between radial position and cross-sectional area. The equation for $\overline{\overline{\theta}}_1$, for example, then becomes

$$\overline{\overline{\theta}}_1 = 2 \sum_{i=1}^{N} x_2^{(i)}\, \overline{\theta}_1^{(i)}/N \qquad (5)$$

For a particular typical sample, the average polar angle calculated from Equations (4) and (5) was 36.7°. This was checked by an independent method in which the orientation of individual fibers is measured by the ellipticity of their cross section in the x_1 plane. Fibers that are in exact longitudinal alignment along the length of the rod cut a perfect circle in the transverse x_1 plane. Oblique fibers appear as an ellipse. The cosine of the polar angle θ_1 for each fiber equals the ratio of the minor-to-major axes. This tedious procedure dealing with hundreds of individual fibers gave an average $\bar{\bar{\theta}}_1$ of 44.7°. Twelve percent of the fibers were in the range 0-30°, with the remaining 84% approximately uniformly distributed between 30° and 80°. Because fibers oriented at $\theta_1 < 30°$ appear as almost perfect circles this method is inaccurate. The check with the previous result within 20% is therefore acceptable.

The measured tensile strengths of several molded rods are correlated in Figure 12 against their $\bar{\bar{\theta}}_1$, which was calculated by integrating over the measured distributions of ϕ_1 and ϕ_3 according to Equation 4, and then summing over the area with Equation (5). The linear correlation not only demonstrates the accuracy of the calculation scheme, but points out that in these long ($\geq$ 1/8") discontinuous fiber composites, fiber orientation is a critical structural parameter affecting tensile strength. This conclusion is discussed more thoroughly in (5). A similar plot of the Young's modulus is shown in Figure 13 for various types of discontinuous fiber composites at a 50 v/o loading.

Summary

The fiber orientation distribution in a molded part can be described in terms of macroscopic and microscopic variations. The former concerns changes in the local mean orientation direction over distances that are large with respect to a fiber diameter and of the same order as the minimum molding dimension. These are the changes in the orientation pattern that are visible to the eye in a plane cut into the molding. In addition, the individual fibers in a microscopic region show a variation about the mean local position, which is the angle displayed by the gross pattern at that point. This breakdown systematizes the study of complex fiber orientation distributions that occur in flow molding.

The microscopic distribution is symmetric and can be taken to be normal. In flow moldings, the macroscopic distribution over the coordinates of the molding is continuous and can be measured and described empirically. Since most injection or transfer moldings are three dimensional in shape, the simpler planar orientation measurements that suffice for laminates are inadequate. Instead, the polar angle about a direction of interest must be measured, or planar measurements must be made in two orthogonal planes throughout the molding and combined. The averaged polar angle around a specified axis taken as the zero direction can be used as an indication of the spread in the orientation distribution. In order to calculate mechanical properties, however, this simple representation will not suffice and it becomes necessary to report the regression of either the polar angle or the component planar angles over the distance coordinates of the molding, along with the associated standard deviations about the regression line.

The problems of dealing with a polar distribution are discussed and it is shown how the simplification into linear statistics can be effected by properly defining the angular domains. This includes the proper treatment of negative and positive angles. Some simplifications result when symmetry is present.

For concentrated suspensions of fibers in a matrix whose viscosity is less than 10^4-10^5 poise, there is no dependence of orientation on coordinate position in the direction of flow through uniform channels. When a cavity is end gated with a small gate so that the melt experiences a volume expansion as it flows into the mold cavity, the fibers turn predominantly transverse to the streamlines. Some rounding of the orientation patterns occurs near the walls; this may be the effect of the entrance geometry, or may result from either wall interaction or shearing stresses. The effects of molding variables are given for a low viscosity (40% reacted) epoxy molding compound. Low viscosity and low flow rate favor a large envelope of nearly longitudinal orientation around the central core, thus changing the overall orientation from its otherwise predominantly transverse nature. Degree of bundle integrity and fiber length (1/8" x 1/4" fibers) have no noticeable effect.

The characterization of orientation in rods is similar to that for rectangular pieces, but is simplified by the higher degree of symmetry present.

Both tensile strength and modulus depend strongly on the overall level of fiber orientation.

Acknowledgment

The author wishes to express his gratitude to Mr. D. J. Morotz and to Miss A. M. Gordon for their assistance in the experimental phases of this study.

This research was supported by the Advanced Research Projects Agency of the Department of Defense and was monitored by the Office of Naval Research under contract no. N00014-67-C-0218.

References

1. Goettler, L. A., SPI, 25th Composites Div. Meeting, Washington, Feb. 1970, Section 14A.
2. Goettler, L. A. and R. E. Lavengood, "Stiffness of Non-Aligned Fiber Reinforced Composites," Monsanto/Washington University ARPA Report, HPC No. 71-141A, 1972.
3. Goettler, L. A., Modern Plastics, 48, 140 (April 1970).
4. Anderson, W. M. and D. C. Morris, SPI 23rd Composites Div. Meeting, Feb. 1968, Section 17-E.
5. Goettler, L. A., "Molding of Oriented Short Fiber Composites I. Ultimate Tensile Properties," Monsanto/Washington University ARPA Report No. HPC 72-149, 1972.
6. Goettler, L. A., "Molding of Oriented Short-Fiber Composites II. Flow Through Converged Channels," Monsanto/Washington U. ARPA Report No. HPC 70-130, 1972.
7. Goettler, L. A., "Molding of Oriented Short Fiber Composites III. Rate Effects on Fiber Alignment in Convergent Channels," Monsanto/Washington University ARPA Report No. 72-150, 1972.

List of Tables

Table 1

Dispersion of Individual Fiber Orientations in 40 v/o fiberglass reinforced epoxy plunger moldings.

Material	s_F, degrees
Hand blended CS308A (bar mold)	15.
Hand blended CS308A (rod mold)	13.
Encapsulated grain (ref. 4)	8.
Commercial epoxy BMC	22.

List of Figures

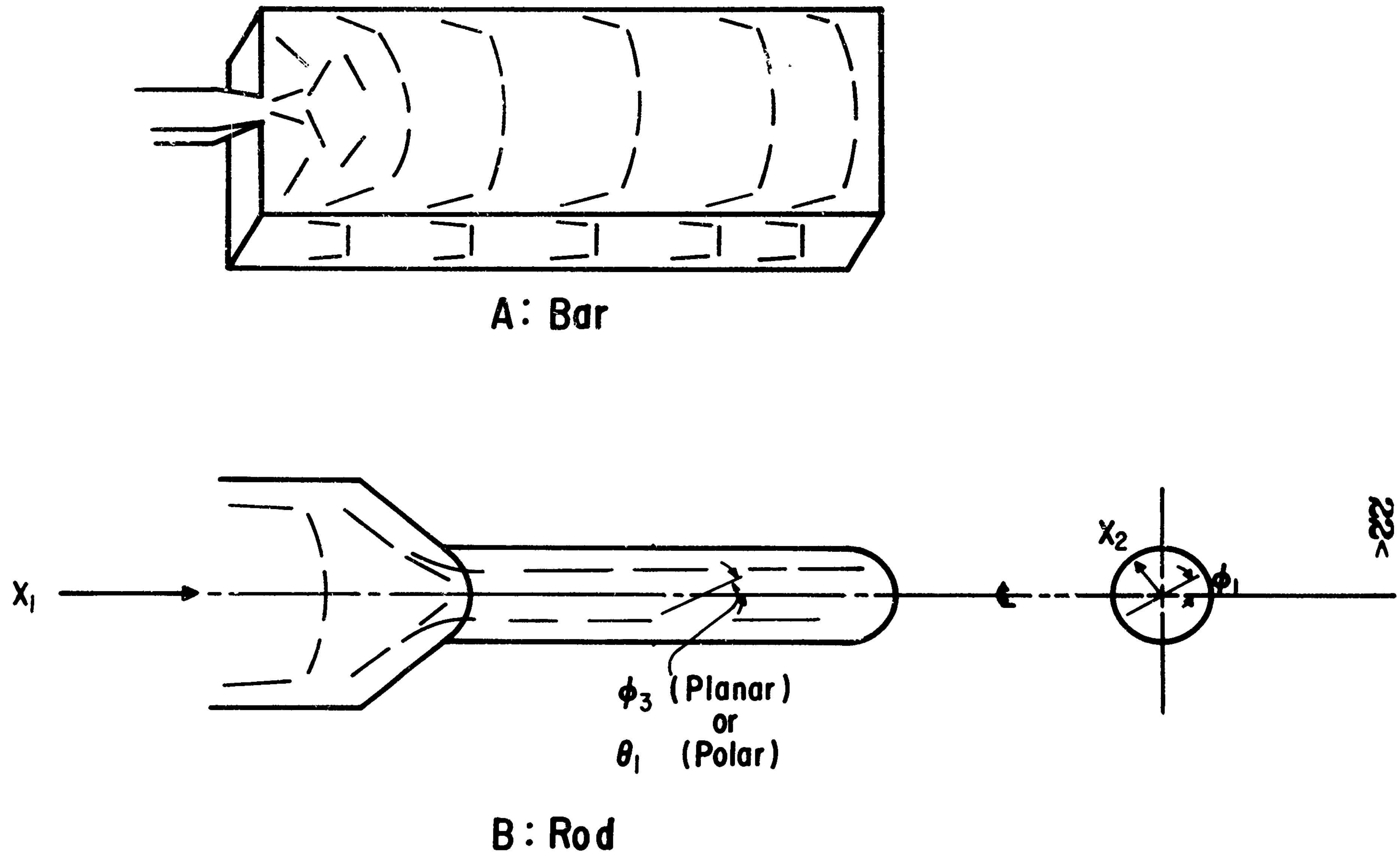

1. Fiber orientation patterns in two simple moldings.

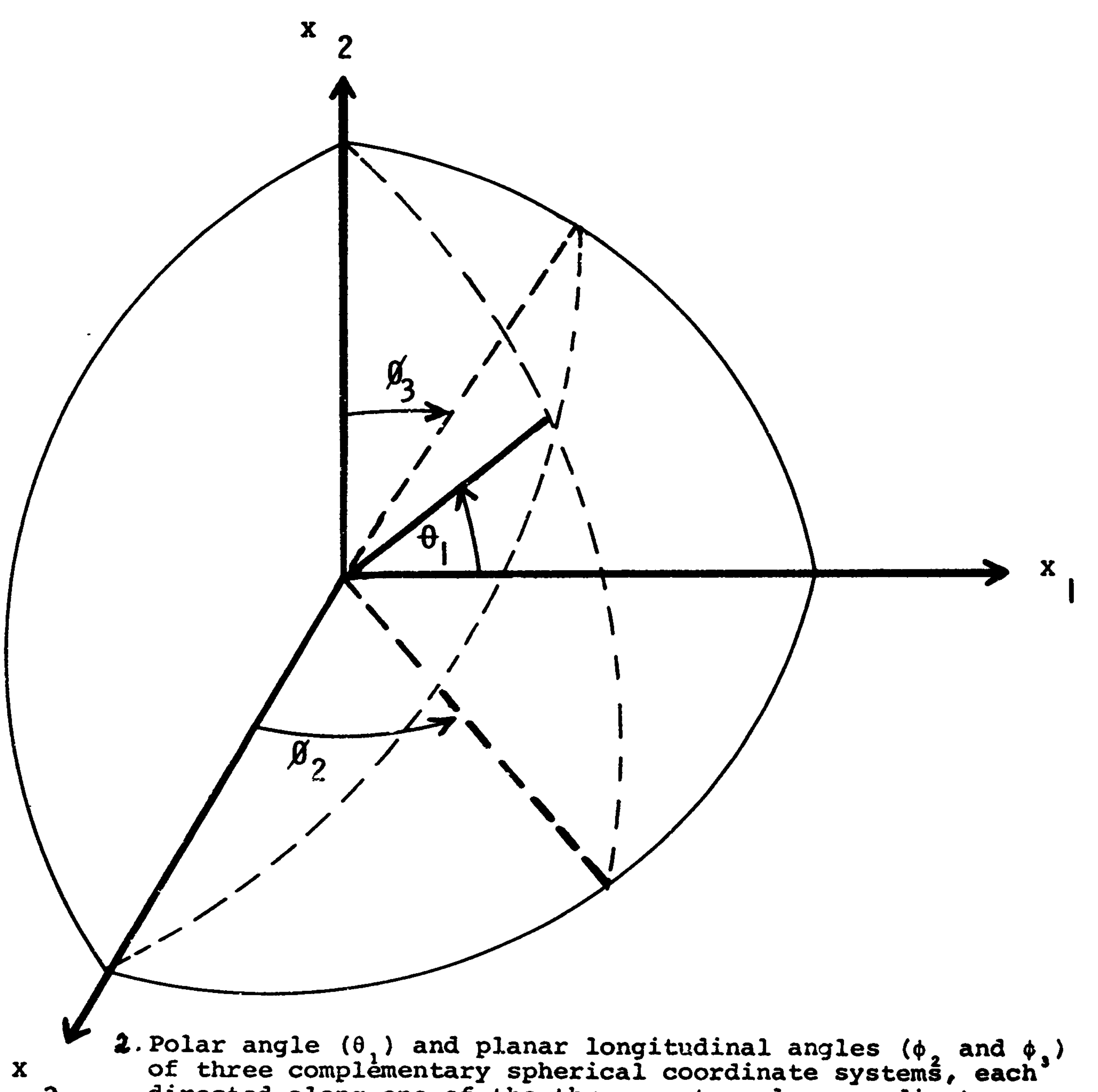

2. Polar angle (θ_1) and planar longitudinal angles (ϕ_2 and ϕ_3) of three complementary spherical coordinate systems, each directed along one of the three rectangular coordinate axes at a point.

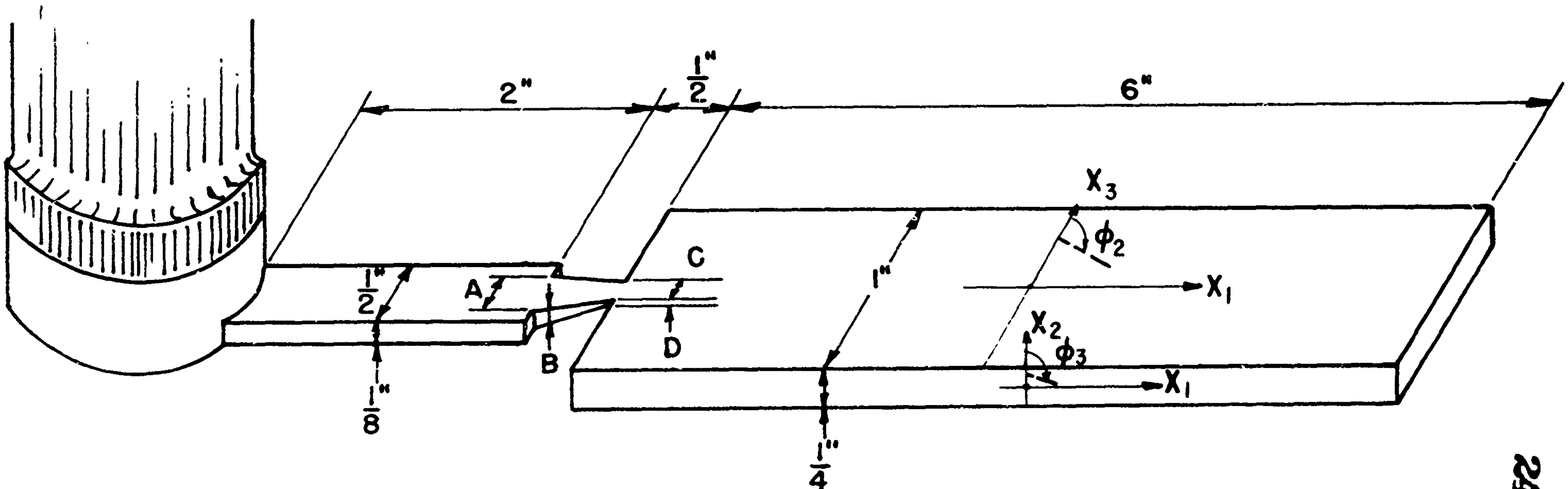

24<

. 3. Geometry for plunger molding of 1/8" CS308A fiberglass reinforced epoxy bars.

Figure 4

Scheme for calculation of average orientation or mechanical property from measured orientation distributions

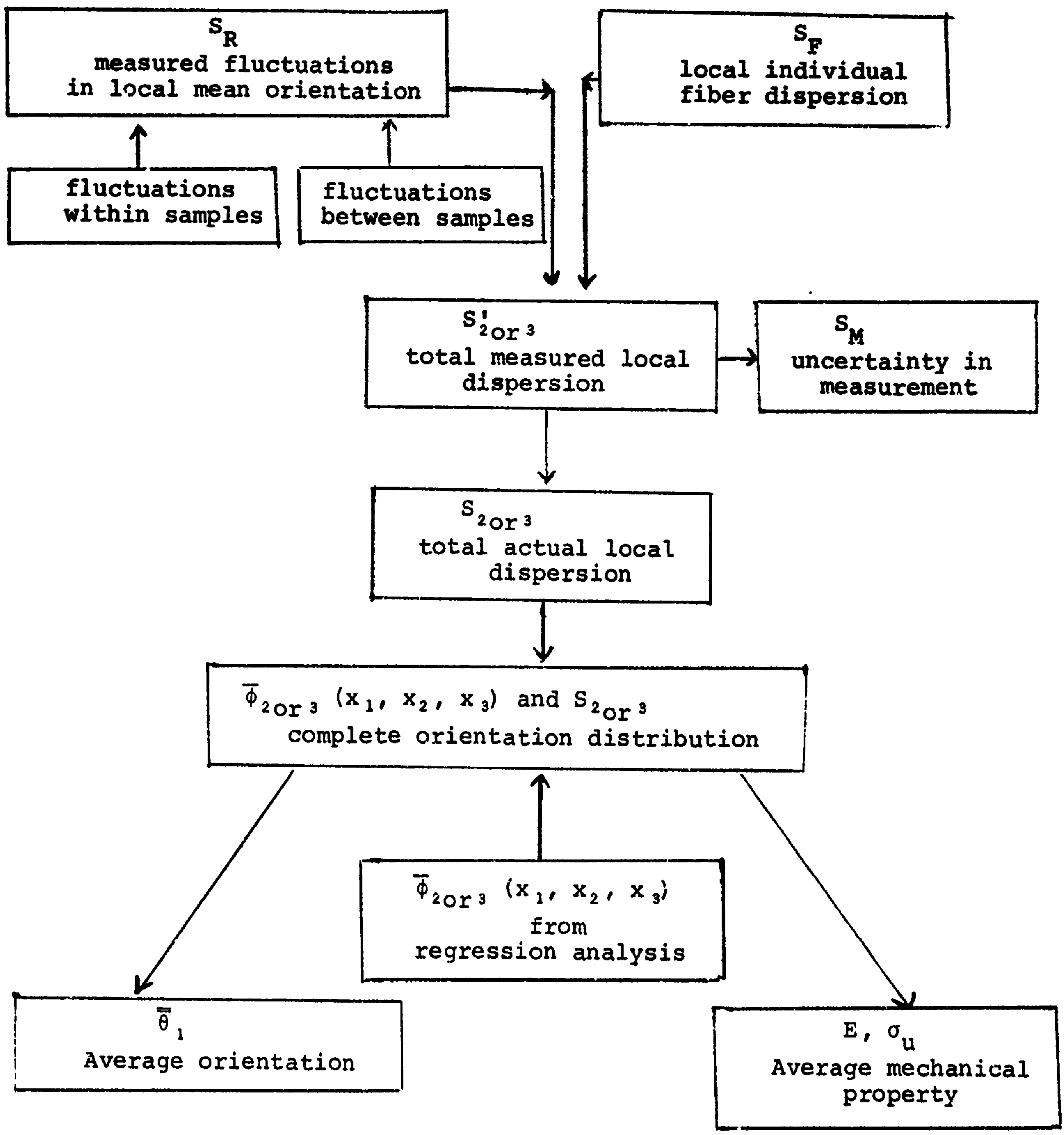

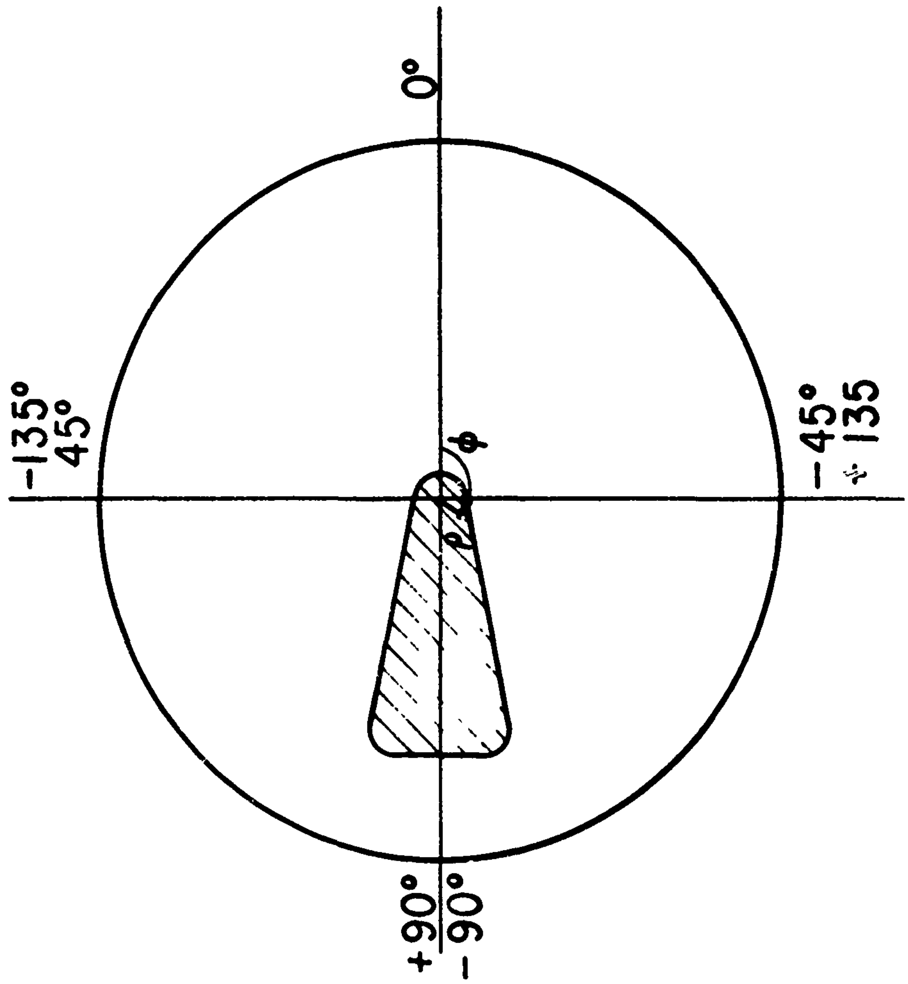

5. Polar representation of orientation distribution.

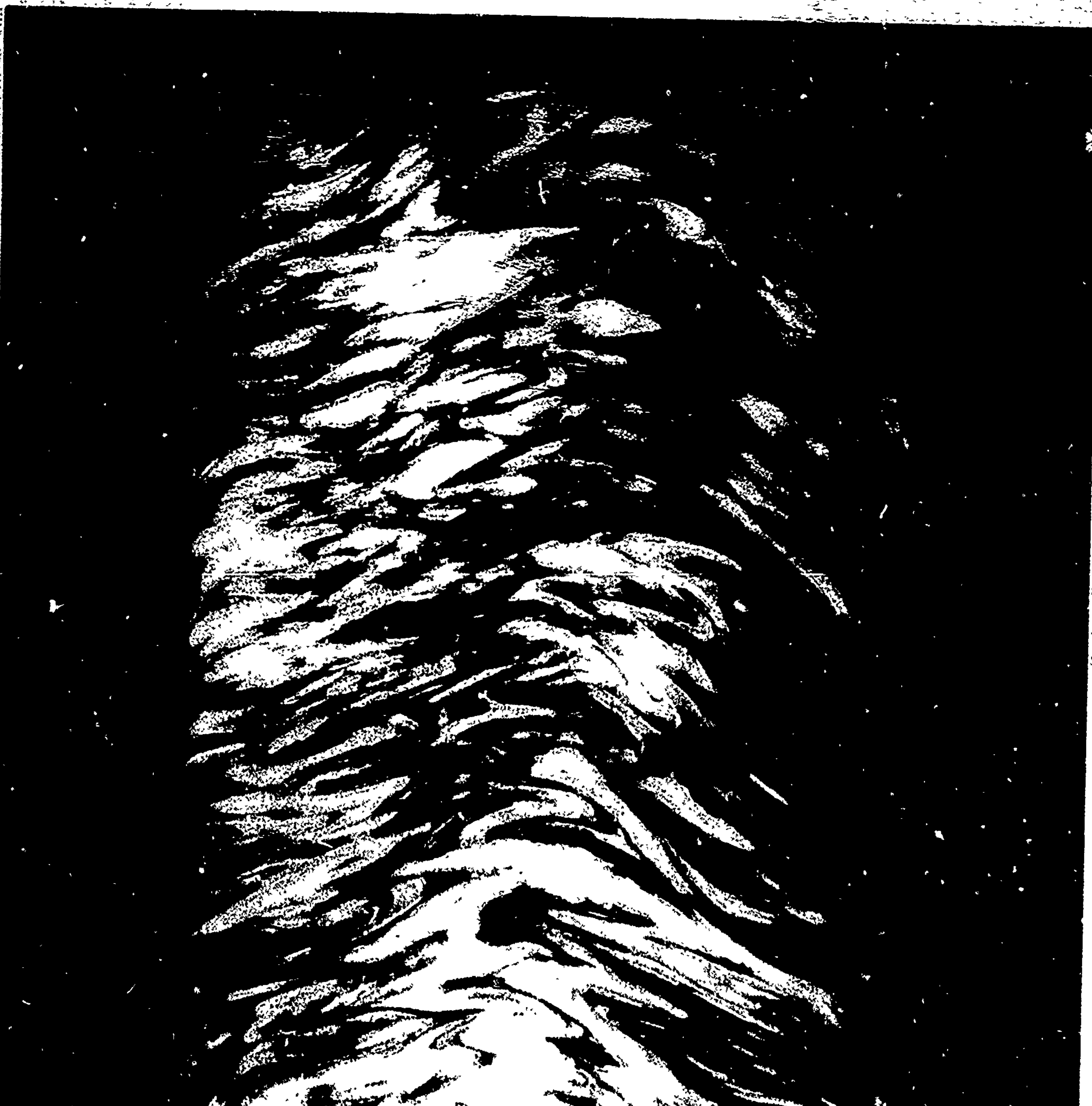

6. Orientation pattern in the x_2 plane of plunger molded fiberglass/epoxy bars.

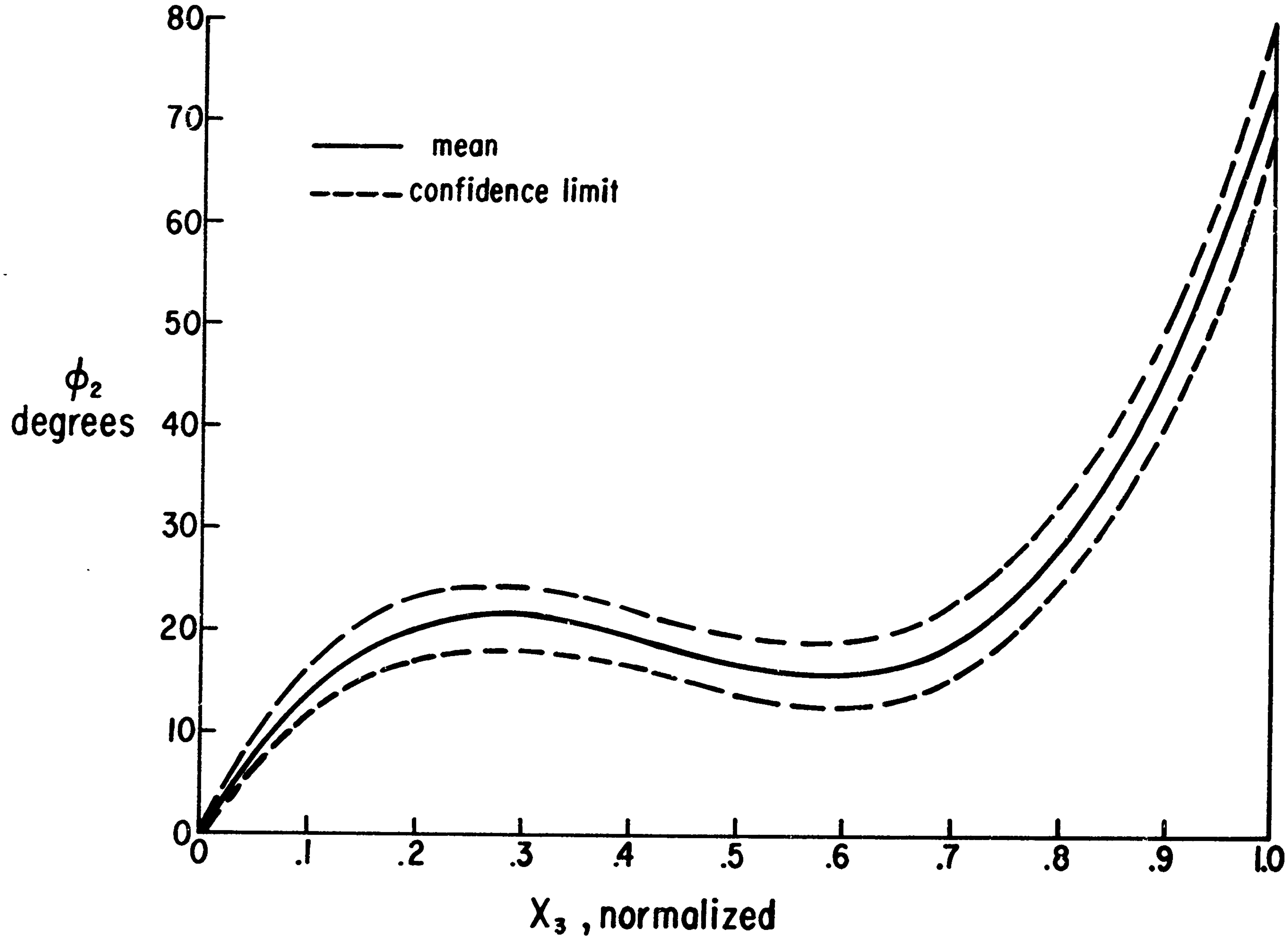

7. $\overline{\phi}_2$ (x_3; x_2 = 0) in an end-gated 1/4" x 1" x 6" bar with 90% confidence interval indicated for a high viscosity molding compound and large ingate.

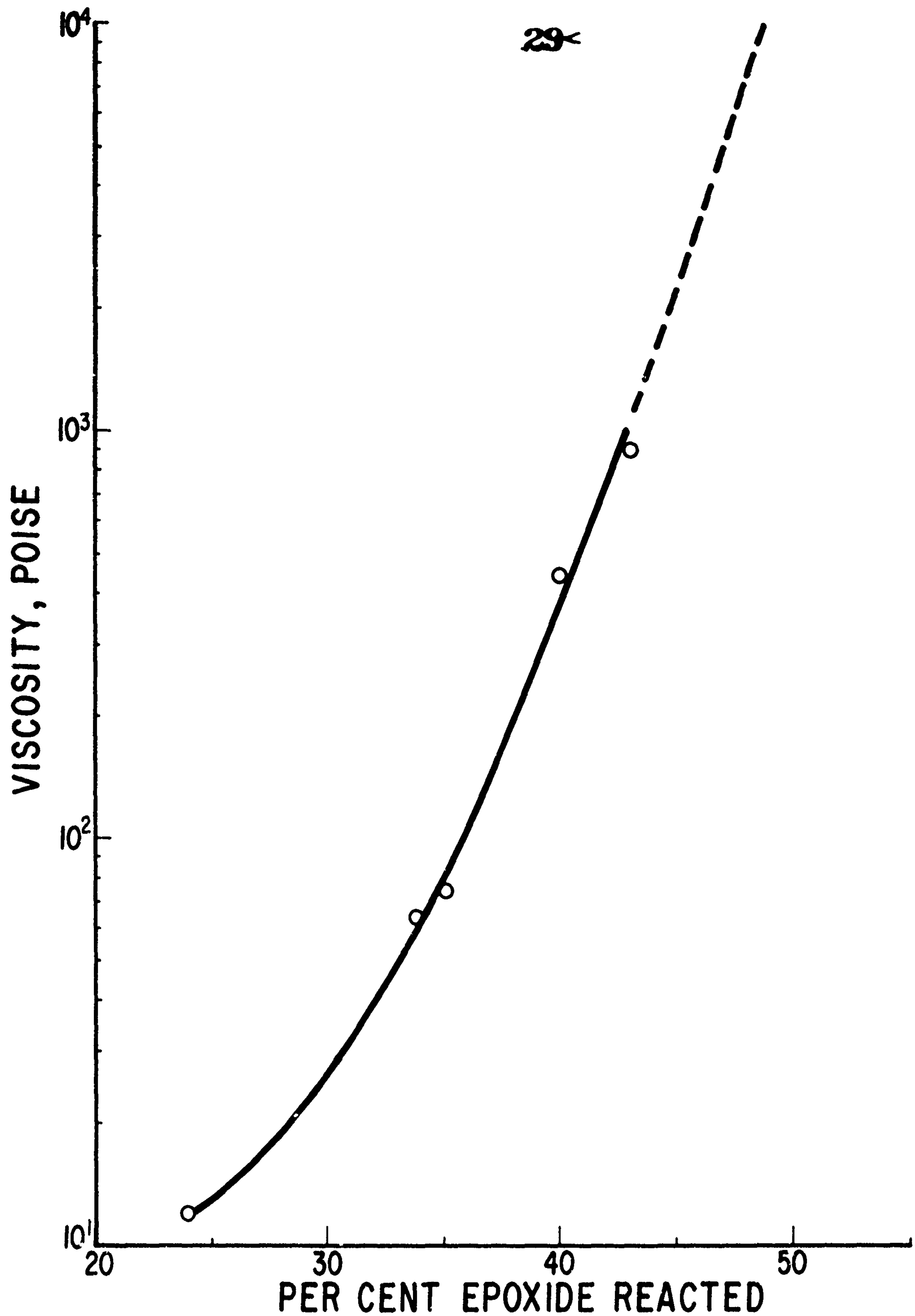

8. Viscosity of epoxy matrix at 110°C.

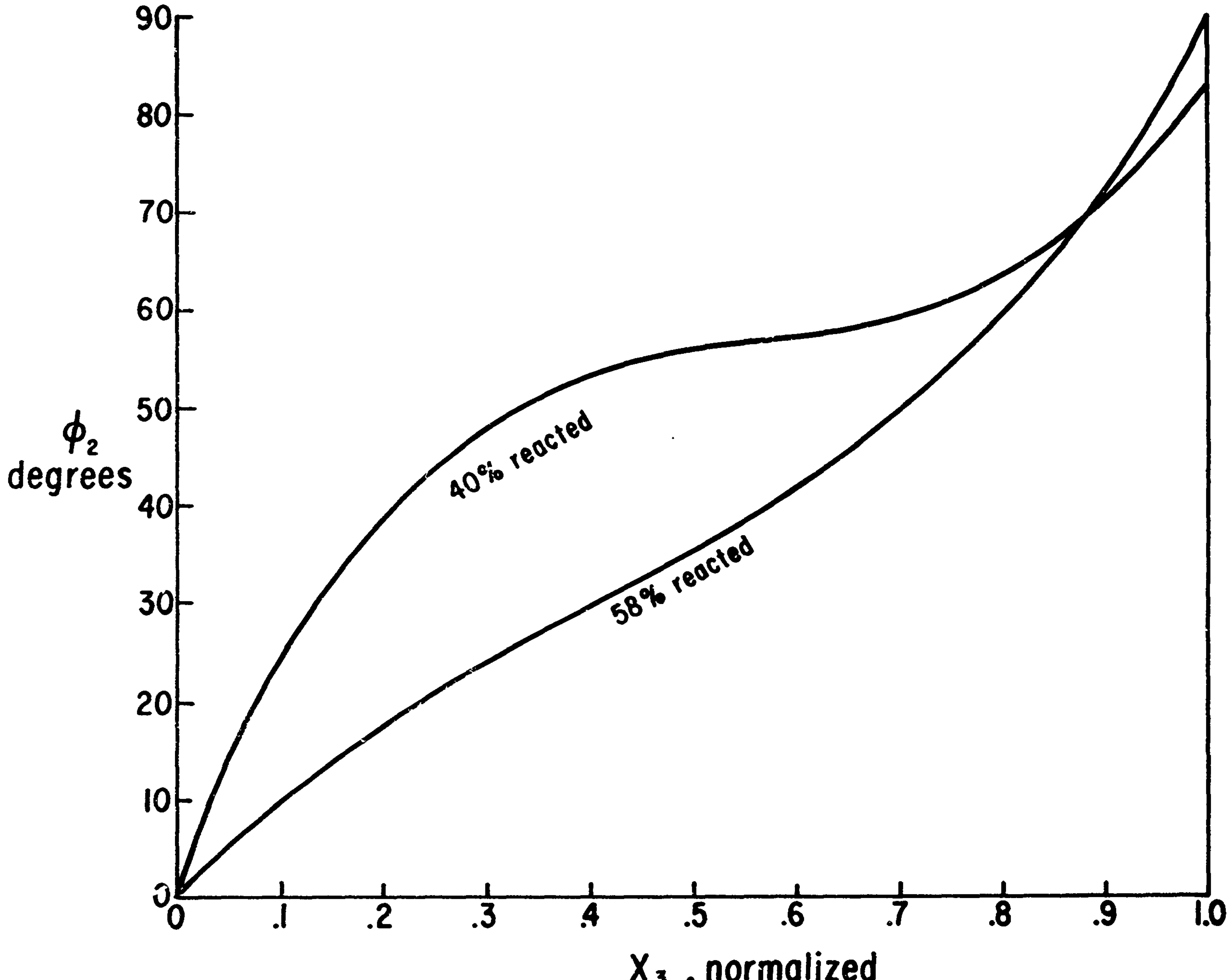

9. Effect of resin viscosity level on orientation in the bar, 40 v/o 1/8" CS308A fiberglass in Epon 828/MDA, 1/4" x .060" end gate.

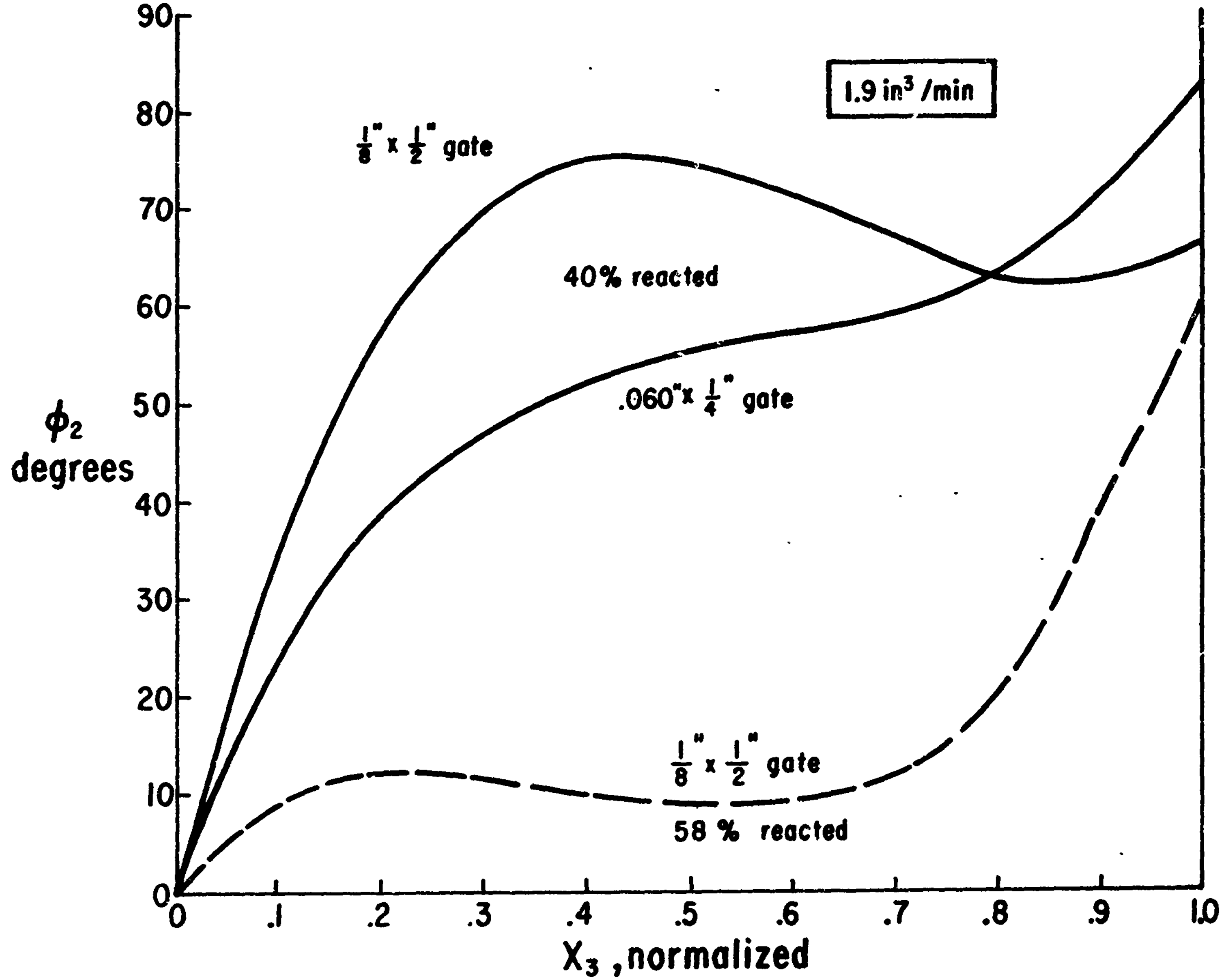

10. Effect of resin viscosity and gate size on orientation obtained for 40 v/o 1/8" CS308A fiberglass.

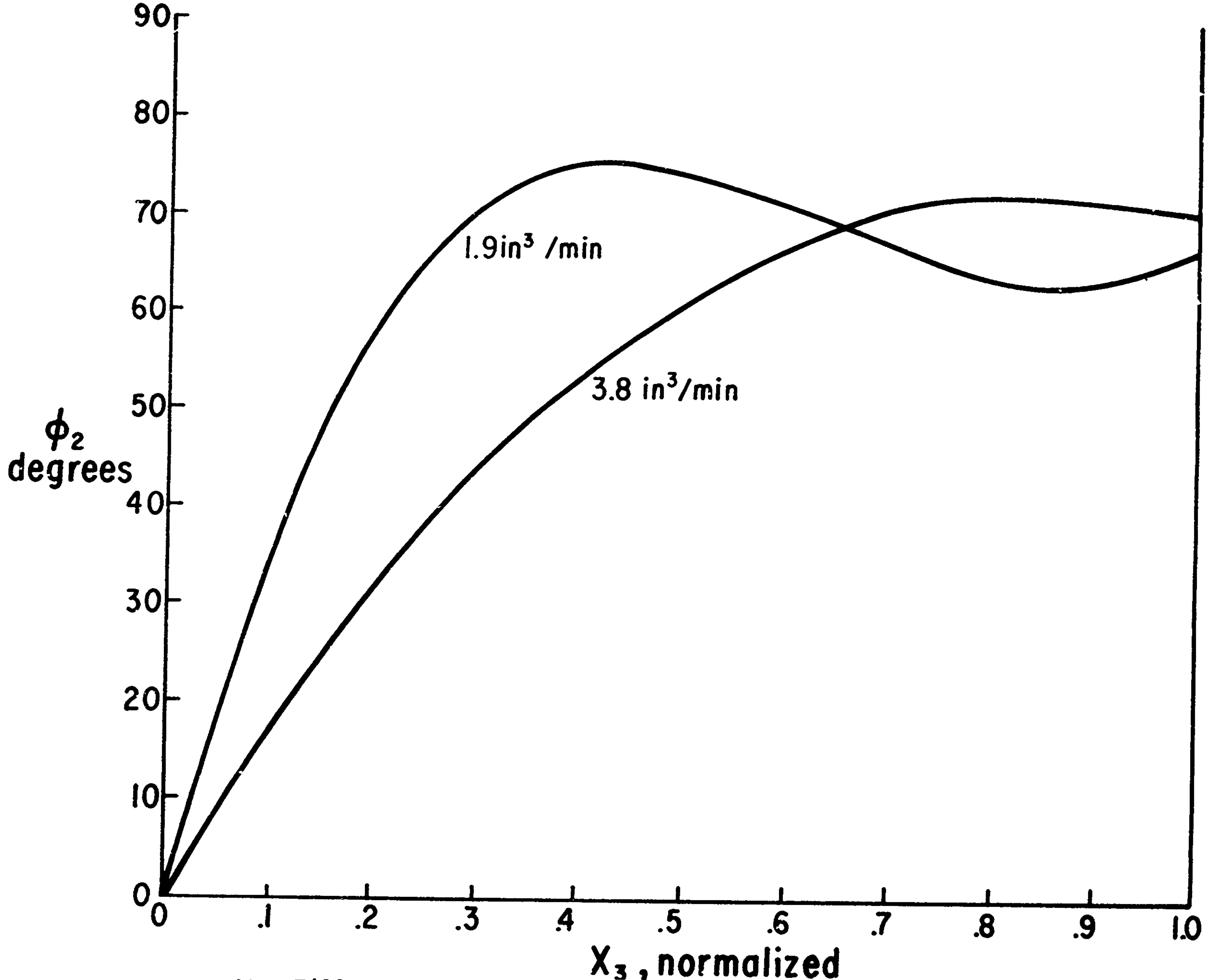

11. Fill rate effects on orientation in a bar molded of 40 v/o 1/8" CS308A in 40% reacted Epon 828/MDA through 1/2" x 1/8" gates.

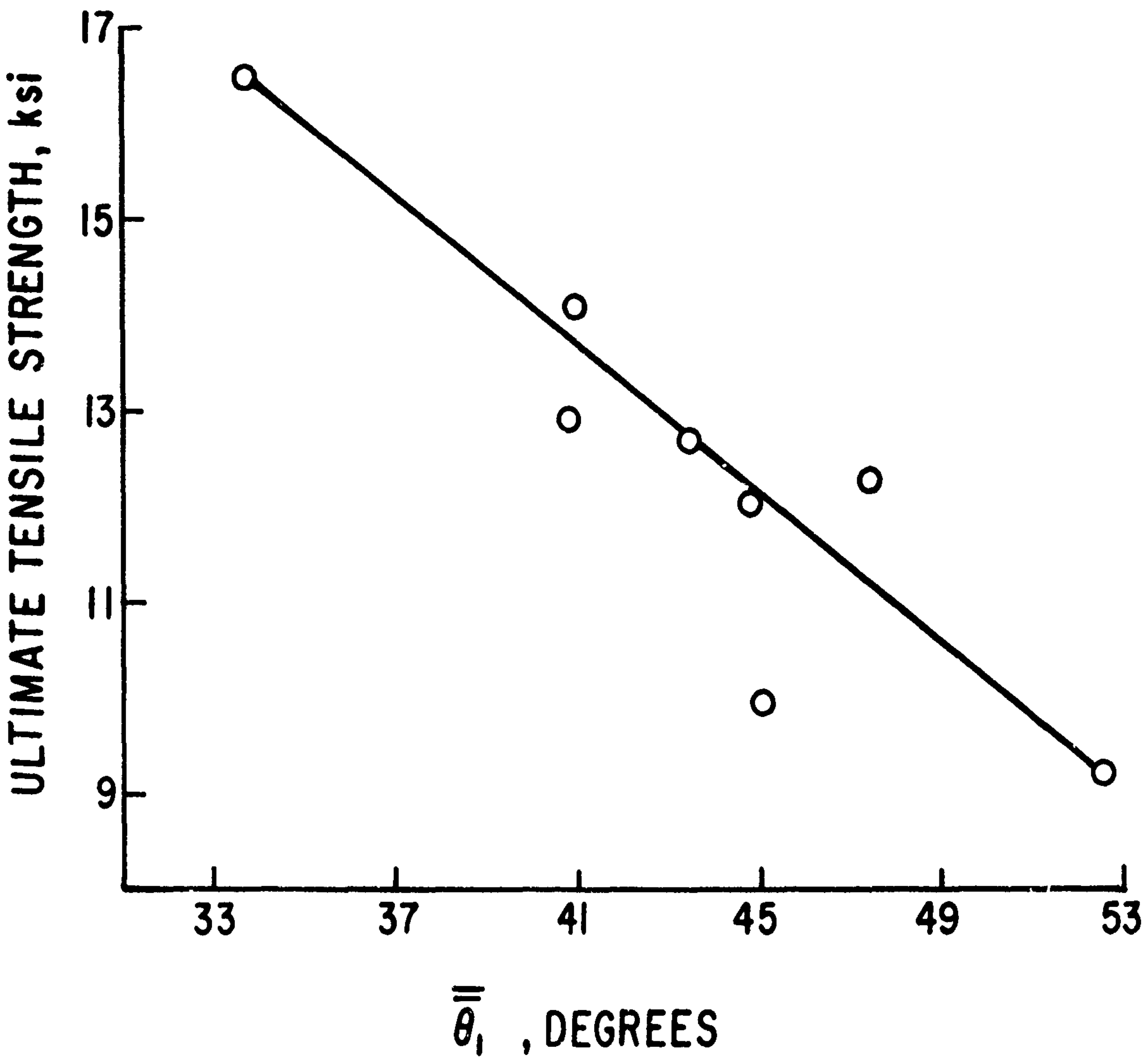

12. Correltation between measured tensile strength and calculated average polar angle for 40 v/o 1/8" CS308A flow molded fiberglass/epoxy composite rods.

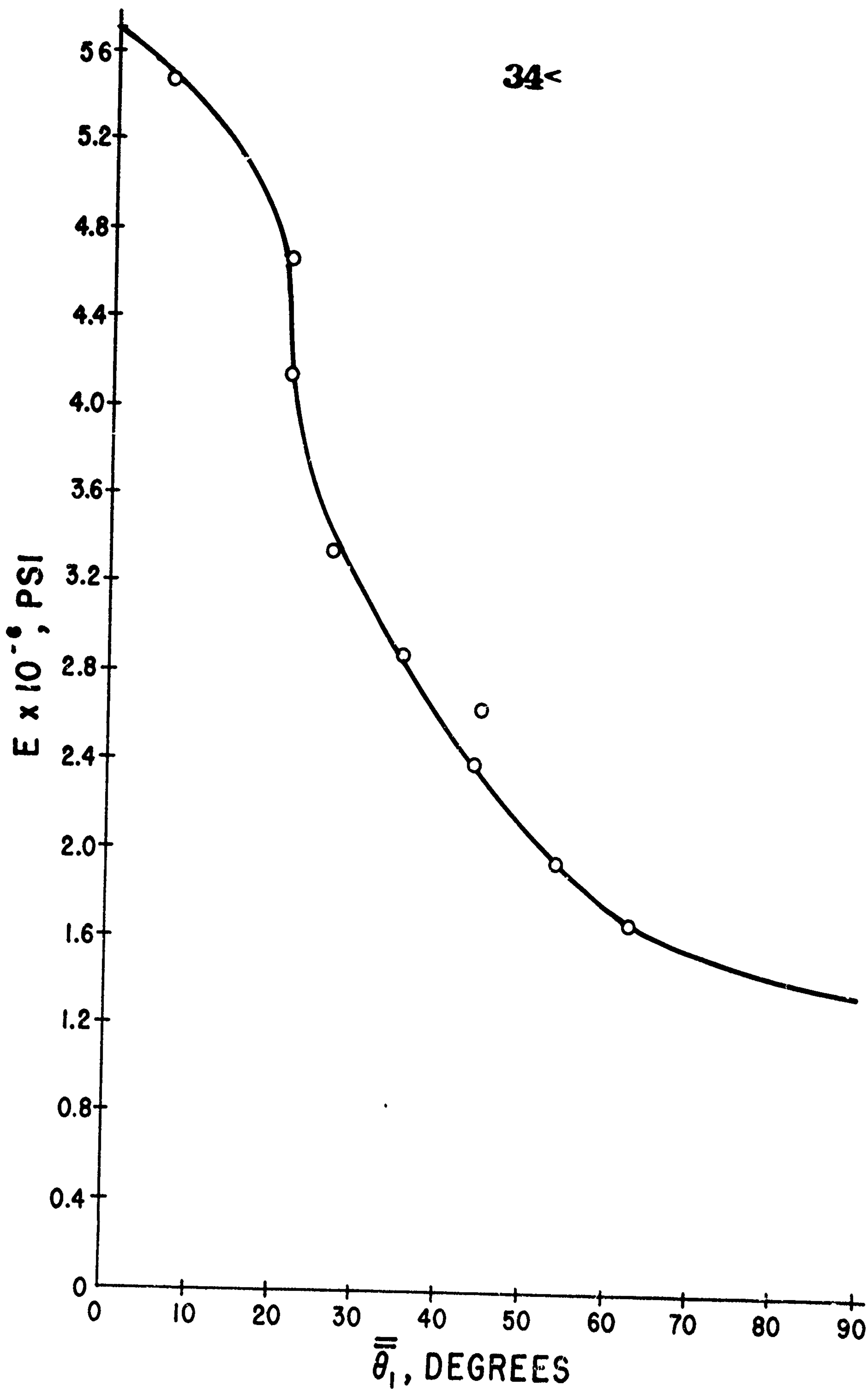

13. Correlation between Young's modulus and calculated average polar angle for various types of 50 v/o discontinuous glass fiber reinforced epoxy composites.